01,05,13

Two- and three-component alloys nanowires: correlation of structural and magnetic properties

© D.R. Khayretdinova[1,2], I.M. Doludenko[1,¶], L.V. Panina[2,3], D.L. Zagorsky[1]

[1] Shubnikov Institute of Crystallography „Crystallography and Photonics“, Russian Academy of Sciences, Moscow, Russia
[2] National University of Science and Technology MISiS, Moscow, Russia
[3] Immanuel Kant Baltic Federal University, Kaliningrad, Russia

¶ E-mail: doludenko.i@yandex.ru

Received April 24, 2022
Revised April 29, 2022
Accepted May 12, 2022

Several types of nanowires (NWs) made of alloys of various compositions obtained by the method of matrix synthesis based on track membranes have been studied. Electrolytes were selected to obtain NWs of the desired composition. The control of electrodeposition by chronoamperograms made it possible to systematically change the geometric parameters and morphology. The topographies of the resulting NW arrays and their elemental composition were studied using electron microscopy with an X-ray spectral analyzer. The magnetic properties of the samples were studied on a vibrating magnetometer. The structures of binary alloys were studied: for NWs of FeCo alloys, the dependence of the coercive force on the composition was studied. The obtained dependence has two maxima — at an equiatomic composition and at a cobalt content of about 90%. For $Fe_{0.3}Co_{0.7}$ NWs, a sharp increase in the coercive force with decreasing diameter is shown. It is assumed that this effect is due to the formation of single-domain crystallites, the processes of magnetization reversal of which are associated with a uniform rotation of the magnetization. For NWs made of FeNi alloys, the influence of the aspect ratio on the coercive force has been proved. Ternary alloys of the FeCoCu system have been studied: it has been shown that the addition of copper significantly increases the coercive force, which reaches a maximum at a copper content of about 5%. The obtained X-ray data suggest that the effect of an increase in the coercive force is associated with the formation of fine-grained inclusions based on copper, which lead to effective deceleration of the domain walls. The data obtained expand the range of possibilities for controlling the magnetic properties of NW arrays obtained by the method of matrix synthesis. Keywords: nanowires, matrix synthesis, microscopy, elemental analysis, magnetic properties, coercive force.

Keywords: nanowires, matrix synthesis, microscopy, elemental analysis, magnetic properties, coercive force.

DOI: 10.21883/PSS.2022.09.54143.24HH

1. Introduction

One of the promising types of nanostructured magnetic materials are nanowire (NW) from iron group metals. Arrays of such NW can be obtained by template synthesis based on porous matrices of different types. Thus, track membranes (nuclear filters) — thin polymer films with identical through-holes of predefined sizes are widely used as growth matrices. The idea of synthesis in this case is that electrodeposition of metals is performed in the pores, during which molds (replicas) of the pore channels are formed. The great advantage of the approach lies in the possibility of independently and widely varying the main parameters of the obtained structures — their geometry, composition, structure and magnetic properties, respectively. However, the connection of many parameters (in particular, the receiving conditions and magnetic properties in one-dimensional nanostructures such as the resulting NW) differs significantly from similar relationships for bulk materials. A number of works are devoted to the study of these relationships and, accordingly, the study of the possibility of controlling magnetic properties.

In general, iron compounds with cobalt or nickel are of great interest because their magnetic properties vary. Thus, FeCo joints can have both hard-magnetic and soft-magnetic properties. In films from this alloy extremely high magnetic anisotropy can occur due to the change of crystal symmetry and the transition to the tetragonal phase jcite1,2. Iron-cobalt alloys of equivalent composition can have maximum saturation magnetization: in a single-domain state, the coercive force H_c can reach several kOe jcite3,4. In general, FeCo alloy NW are candidate materials (instead of rare earth metals magnets) for permanent magnets (for example, to create magnetic recording devices). Iron-nickel alloys and their nanostructures are often used as magnetically soft material with low magnetostricity and high saturation magnetization. NW based on them are often textured and have high anisotropy [5–8].

In works [9,10] FeCo-NW with diameters from 100 to 300 nm were grown in the pores of aluminum oxide (POA), their structure and magnetic properties were studied. The authors of [11,12] described obtaining different FeNi-NW diameters in the POA pores, as well as their structure, electrical and magnetic properties. In work [13] NW from FeCo were studied (metal ratio in electrolyte $Fe:Co = 3:1$), obtained by electrodeposition into the pores of track membranes with diameters from 30 to 200 nm. The growth was carried out at different potentials: from 600 to 900 mV. The dependence of structural data and the Mössbauer spectra on the conditions of obtaining is shown. In work [14] NW from FeCo and FeNi alloys were synthesized in track membranes with pores of 30 to 200 nm at voltages of 600 to 800 mV. It is shown that both the growth voltage and pore channel diameters influence the magnetic properties of the received NW. In work [15] FeNi-NW with diameters 30 and 70 nm are obtained. The dimensions of magnetic domains (about 20 nm) have been determined and the orientation of their magnetic moments along the NW axis has been shown.

In previous works of the authors NW of double alloys based on iron have been studied. In work [16] it has been shown that the structure and magnetic properties of NW arrays depend on changes in electrolyte composition and/or deposition conditions.

In [17] it is noted that when FeNi-NW grows, there is a so-called anomalous iron co-deposition: the amount of iron in the NW is significantly higher than in the electrolyte. The elemental composition of the NW in this case changes in its length. In addition, the NW composition and the distribution of the elements by length strongly depends on the growth voltage — reduction of the latter leads to an integral increase in the iron content and increase in the composition differences in different parts of the NW. For FeCo-NW, these dependencies are much weaker. Thus, the elemental composition of these NW almost coincides with the composition of the electrolyte and changes little when the growth voltage changes.

The X-ray crystalline analysis showed that the structure of both types of NW is solid solutions of two metals [18]. For iron-containing NW of more than 20−25% there is an iron-based BCC lattice. At low iron concentrations, a structure with a BCC lattice (nickel or cobalt based) is formed. It is also shown that in all cases, when the concentration ratio changes within one phase, the parameter of the lattice changes accordingly to the metal concentration ratio.

The presence of iron in the samples allowed the use of the Mössbauer spectroscopy to estimate the magnetic characteristics of NW [16]. The resulting spectra prove the spontaneous magnetization of the NW primarily along their axes. According to the ratio of the intensity of the sextet lines, the angles between the axis of the NW and the direction of magnetization are determined: it is shown that at small diameters the magnetization vector is directed practically along the axis of the NW. For the first time, the value of the ultrafine magnetic field on the core (Bhf) was determined and the dependence of this parameter on the composition of the NW was studied. It is shown that FeCo-NW has higher Bhf values than FeNi-NW. For both types of NW, the Bhf parameter increases with the relative iron content and is close to the values of cubic crystals.

The study of dependence of magnetic properties of FeCo-NW samples on their composition [19] has begun. The non-linear nature of this relationship is shown: a basic maximum of H_c is found for samples with equiatomic composition (as well as for bulk samples). For FeNi alloy NW specimens, a H_c dependence on the diameter was found: a decrease in the diameter of the NW was shown to bring the specimen parameters (usually soft-magnetic) closer to hard-magnetic.

Note that there are other methods for changing magnetic characteristics. Thus, a number of papers describe the possibility of increasing H_c by introducing a non-magnetic element, such as copper.

In a series of works NW were obtained on the basis of FeCoCu alloy. It is known that in bulk materials such a reception (introduction of a non-magnetic impurity) can lead to the creation of structural defects that lead to slowing down the movement of domain walls. In all cases, an aluminium oxide matrix was used. In work [20] formulations with a copper content of more than 10% have been studied, and it has been shown that H_c decreases with this concentration. In work [21] NW with a diameter of 18−27 nm and a copper content of 5% were obtained and investigated. It is shown that the value of H_c is quite large already in the original state (0.26 T) and increases significantly when annealing (at 500°) — to 0.36 T. In work [22], NW of the same composition were studied, but with copper segments. The influence of relative thicknesses of copper and magnetic layers on the magnetic properties of the NW array is shown. In work [23] in the NW of FeCoCu alloy with the modulated wall thickness discovered experimentally and described in the model the blast wall pinning effect on „thickening“ NW. It should be noted that in these works X-ray crystallographic studies were carried out, which showed that the structure was single-phase, and in most cases — BCC.

In general, nanoparticles with high H_c can be used in permanent micro-magnets to create magnetic memory devices.

Another, opposite, problem is related to the reduction of H_c. By tasks that require nanoparticles with a small H_c, one can include targeted drug delivery and/or the creation of microheaters powered by variable magnetic field (hypertermium) [9.24]. It is known that another method of varying coercive force (in addition to the composition of the material described above) is a change in geometric parameters.

Analyzing the above data, it is possible to conclude that the method of matrix synthesis opens wide possibilities for the creation of nanoparticles (nanowires) with a variety of properties. However, the relationship between growth parameters, structure and magnetic properties are often not fully identified. So, it is of great practical interest to

create materials with adjustable values of H_c — both high and low. The study of FeCo and FeNi double alloys as well as FeCoCu triple alloy continues in this work. The possibilities of increasing or decreasing H_c due to both controlled composition change and geometric parameters are investigated.

2. Experiment and results

2.1. Materials and instruments

Nanowire arrays were produced by matrix synthesis using track membranes as growth matrices. The membranes were obtained from the Joint Institute for Nuclear Research, Dubna. They were made of polyethylene terephthalate by irradiation by a stream of heavy ions and subsequent etching of the formed latent tracks. The pore diameter ranged from 30 to 200 nm, and the pore density was ranging from $5 \cdot 10^8$ to $9 \cdot 10^9\,\mathrm{cm}^{-2}$, with a matrix thickness of $12\,\mu$m.

Electrochemical deposition was used to fill the pores. For this purpose, one side of the matrix was covered with a continuous conductive copper layer, which served as a precipitation cathode (and also held the wire in case of subsequent removal of the matrix — for example, for microscopic studies). The application of this layer took place in two stages. At the first one vacuum thermal copper was sprayed, resulting in a layer of 50–70 nm. At the second — dust layer was galvanized to a thickness of $4\,\mu$m.

Electrolytes of various compositions were used for the electrochemical deposition of metals, mainly on the basis of sulfate salts of the respective metals.

The following electrolyte composition was used to produce the NW from an iron-cobalt alloy: $CoSO_4 \cdot 7H_2O$ — 16 g/l; $CoCl_2 \cdot 6H_2O$ — 40 g/l. $FeSO_4 \cdot 7H_2O$ ranged from 4 to 72 g/l, which corresponded to a change in the iron-to-nickel ratio from 6 to 53%. In order to increase the relative iron ion concentration, the concentration of cobalt salts decreased in the following sequence: $CoSO_4 \cdot 7H_2$ — 12, 4, 2 g/l; $CoCl_2 \cdot 6H_2O$ — 32, 24, 16, 8 g/l. This technique allowed varying the relative iron ion concentration from 59 to 91%.

The following electrolyte composition was used to produce the NW from an iron-cobalt alloy: $NiSO_4 \cdot 7H_2O$ — 16 g/l, $NiCl_2 \cdot 6H_2O$ — 40 g/l, $FeSO_4 \cdot 7H_2O$ — 8 g/l.

To obtain the NW from the triple alloy — FeCoCu — sulfate salts were used: $CoSO_4 \cdot 4H_2O$ — 51 g/l, $FeSO_4 \cdot 7H_2O$ — 48 g/l, to vary the amount of copper, the amount of copper sulfate ($CuSO_4 \cdot 5H_2O$) varied from 0.5 to 5 g/l.

All electrolytes used the same additives: boric acid — 25 g/ was added as a buffer additive and to maintain the acidity of the electrolyte near the working zone; to prevent Fe^{+2} transition to the trivalent state ascorbic acid (1 g/l) was added in the electrolyte; sodium lauryl sulfate was used as a wetting agent.

The process of electrodeposition was carried out in a galvanic cell (production of the special design bureau of RAS IR), the current source was the potentiostat-galvanostat ELINS P-2X. Iron was used as an anode for the deposition of double alloys, copper was used for the deposition of triple alloys. The process was conducted in potentiostatic mode at 1.5 V for double alloys and 1.8 V for triple alloys. In the galvanic deposition process, time-dependent chronoamperograms were recorded. The latter allowed to control the process, avoiding the scalled „overgrowth“–„output“ of growing metal outside the pore space. („Overgrowth“ was evidenced by an increase in current. Further deposition in such a case would result in the undesirable formation of so called „hats“).

After the samples were collected, they were examined by electron microscopy using the JEOL JSM 6000 plus microscope with an elemental analysis detachable device. The accelerating voltage was about 15 kV, and studies were carried out in both secondary and elastic reflected electrons. Note that for SEM research the polymer matrix was removed in a concentrated solution of alkali.

Magnetometry was conducted on the BM-07 instrument. The measurements were made in two positions: magnetic field along the nanowire, which corresponds to the out-of-plane (OOP) direction, and across the nanowire — to the in-plane (IP) direction. The field ranged from −8.2 to 8.2 kOe.

3. Results and discussion

3.1. Study of the NW growth process

Examples of estimated potentiostatic curves obtained $I(t)$ for the growth of iron-nickel and iron-cobalt-copper alloy arrays are presented in Fig. 1.

Comparison of the graphs shows that the NW growth curves of two-component and three-component alloys are similar. In general, there are several stages described by many authors — initial transition process, growth of the NW within the pore, release of the growing metal beyond the pore, formation of a solid metal layer on the outer surface of the membrane and its subsequent growth. The resulting estimation curves allow to determine the time of full filling of the pores to stop the process at the right moment.

Another way of controlling the length of synthesized NW was to calculate previously obtained formulas. For example, when depositing NW Fe-20%-Ni-80% (permalloy) into a matrix with pore diameters of 100 nm, time was controlled according to the formula obtained in [25]

$$H = 4 \cdot 10^{-9} t^3 + 3 \cdot 10^{-5} t^2 + 0.0128t,$$

where H — length of the NW in μm, and t — time of growth in seconds.

Note that in order to avoid unwanted „overgrowth“ the process was conducted with a „reserve“ of 10% — i.e., after about 90% of the time calculated for full pore filling.

Table 1. CoFeCu-NW compositions

Element	1	2	3	4	5	6	7	8
Fe, at.%	50.2	54.78	59.55	55.125	52.495	56.59	53.17	63.62
Co, at.%	34.96	30.58	35.4	39.75	42.005	40.41	1.005	33.56
Cu, at.%	14.84	14.63	5.05	5.13	5.5	3	5.83	2.83

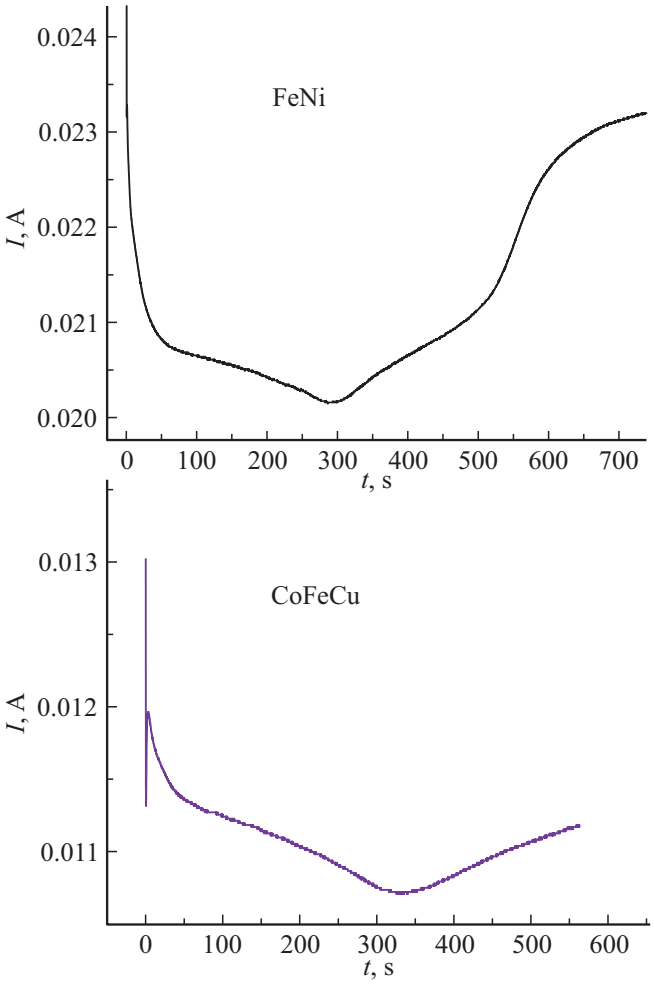

Figure 1. Chronoamperograms of FeNi (FeCo) and FeCoCu nanowire samples growth. The current value refers to the area of the sample (membrane) at 2 cm^2, at the membrane porosity being 5%.

3.2. Elemental analysis microscopy

After synthesizing NW arrays, their SEM images were obtained. Examples of microphotographs are presented in Fig. 2.

Analysis of the resulting microphotographs showed that almost all pores were filled with alloy. The obtained NW in the array have a small length range, the average length is 6.5 μm. The NW diameter is 110–120 nm, which is slightly larger than the diameter of the pore matrix. One reason for this may be the oxidation of the samples in the air after the growth matrix has been removed, resulting in the formation of an oxide layer on the surface of the NW. The assumption is supported by elemental analysis: 3–7 at.% of oxygen is detected on almost all the samples. (Note that oxygen is excluded from the tables below to establish a more accurate relationship between various metals).

The elemental analysis results for triple alloy samples are presented in Table 1.

Comparison of the table data with the composition of growth electrolyte (above) shows the mutual influence of metals. In all cases, the so-called anomalous iron co-precipitation is observed: the Fe fraction in the NW is markedly greater than Fe fraction in the electrolyte. At the same time, increasing the amount of copper reduces this effect. The amount of copper itself in the NW significantly exceeds its quantity in the electrolyte.

Analysis of the X-ray data obtained indicates two phases. This is probably due to the arrival of the copper phase. (Note the preliminary nature of the data obtained: due to the overlap of peaks, the parameters of both lattices have not yet been precisely determined.)

3.3. Magnetic measurements

Hysteresis loops were obtained and investigated for the studied samples, from which the main magnetic parameters were determined, such as H_c and the ratio of residual magnetization M_r to magnetization saturation of M_s (quadratic parameter $SQ = M_r/M_s$. Fig. 3 shows characteristic hysteresis curves for FeNi-NW with a diameter of 100 nm and different lengths, which are characterized by small SQ values for both magnetic field directions. As the length (and aspect ratio) increases, both parameters increase, with H_c being a little larger for perpendicular magnetization (see Table 2).

The presence of grains with a crystallographic axis in the transverse direction may cause this behavior. Small SQ values for short NW are most likely due to the influence of the domain end structure. Cone-shaped domains with

Table 2. The amount of H_c for FeNi-NW with diameter of 100 nm with different length for two directions of magnetic field

Length of NW, μm	ϵ (aspect relation)	$H_{c\parallel}$, Oe	$H_{c\perp}$, Oe	$SQ_\parallel$	$SQ_\perp$
0.98	9.8	73	93	0.03	0.04
1.6	16	106	190	0.07	0.14
4	40	112	247	0.09	0.14

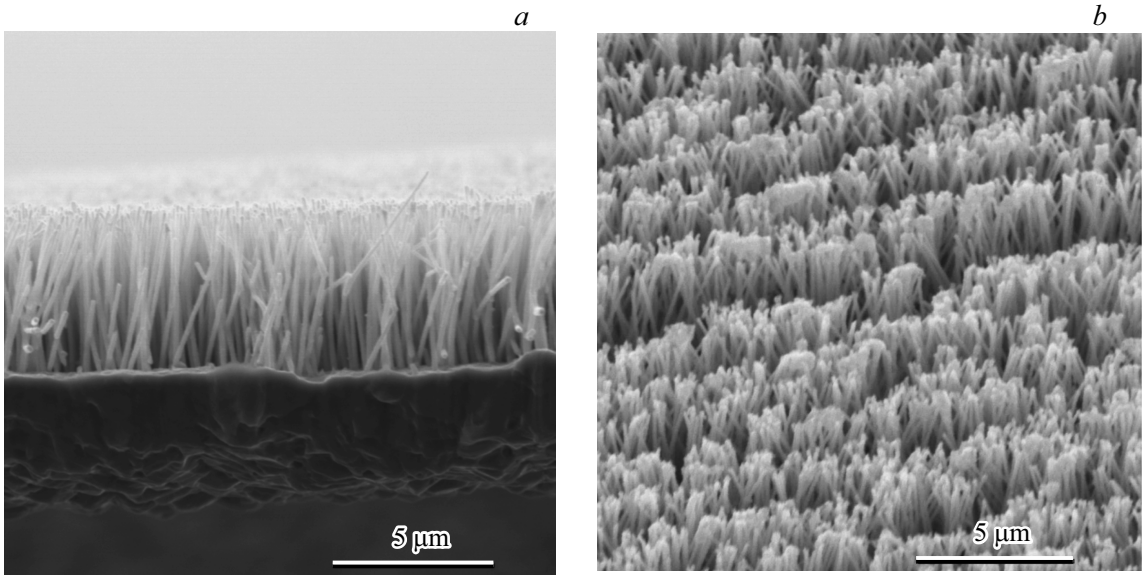

Figure 2. SEM images: *a* — NW from FeNi; *b* — NW from CoFeCu.

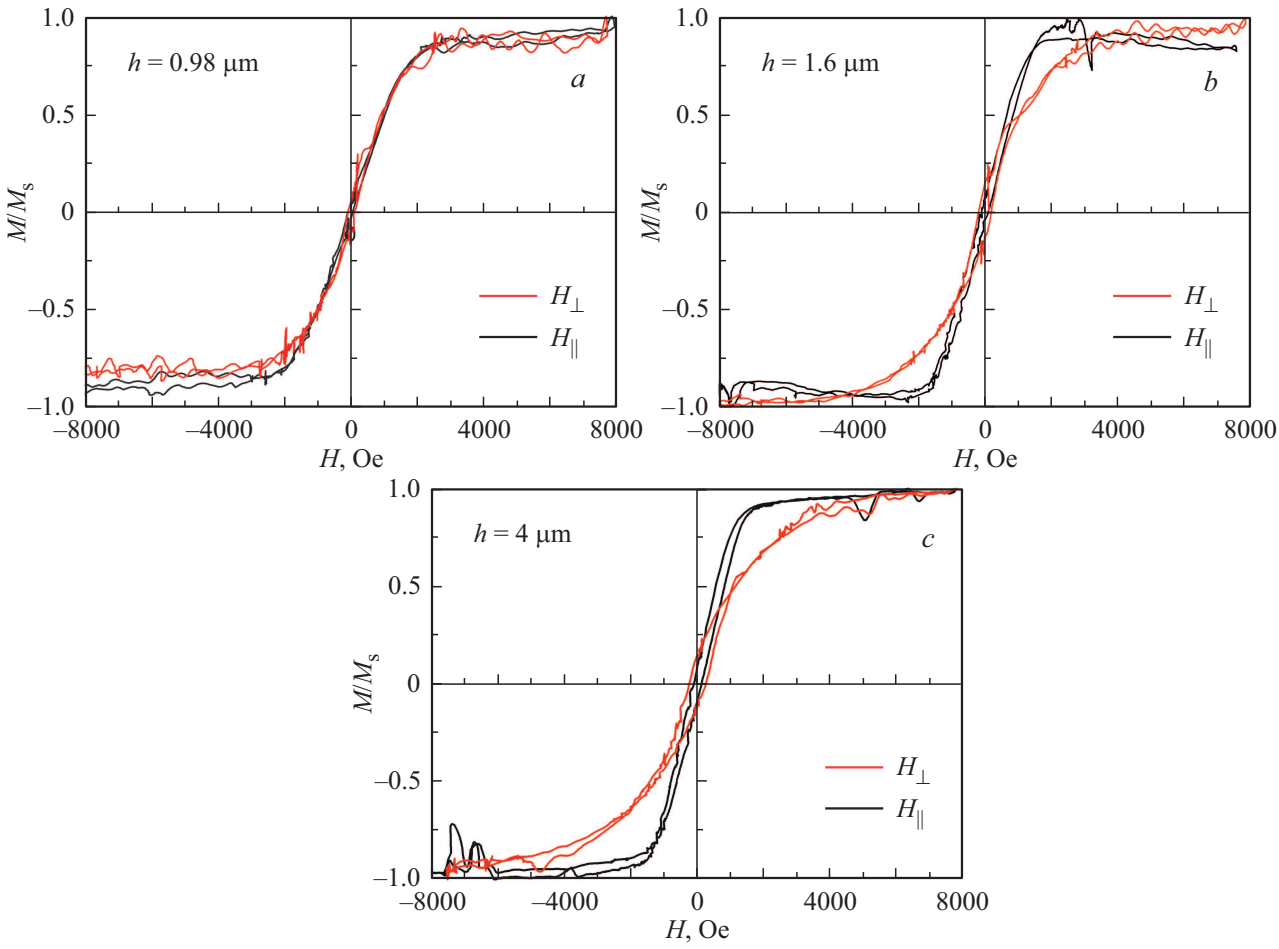

Figure 3. Hysteresis curves for FeNi-NW with a diameter of 100 nm and different lengths: *a* — 0.98 μm, *b* — 1.6 μm, *c* — 4 μm. The black curves — the magnetic field is directed along the wires ($H_{\parallel}$), the red ones — in the perpendicular direction ($H_{\perp}$).

Table 3. The value of H_c for FeNi-NW of various diameters and lengths on the order of 6.5 μm for two directions of external magnetic field $H_{\parallel}$ and $H_{\perp}$

Diameter	Length NW, μm	ϵ (aspect relation)	$H_{c\parallel}$, Oe	$H_{c\perp}$, Oe	$SQ_{\parallel}$	$SQ_{\perp}$
30	7.5	250	700	950	0.82	0.64
70	6.5	93	420	850	0.63	0.62
100	6	60	110	120	0.08	0.05

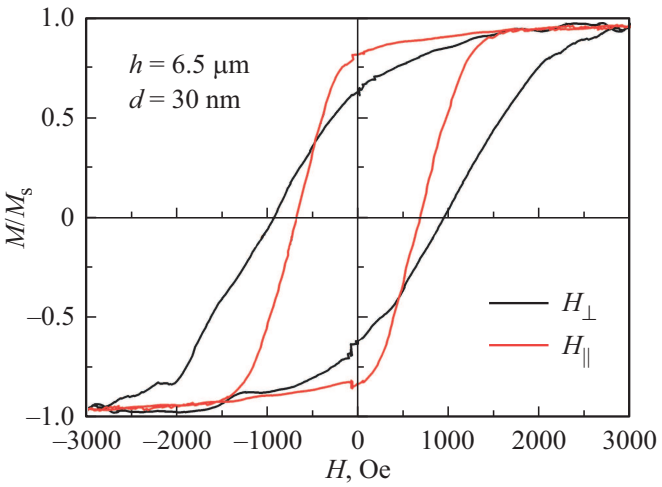

Figure 4. Hysteresis curves for FeNi-NW with a diameter of 30 nm and a length of 6.5 μm for two directions of external magnetic field $H_{\parallel}$ and $H_{\perp}$ (red and black curve, respectively).

opposite magnetization can be formed at the ends of the NW to avoid poles on the surface.

When the diameter of the NW is reduced to 30 nm, there is an increase in coercivity, as shown in Fig. 4. This is due to the formation of a similar single domain state (the critical size of single-domain Ni is about 20 nm). Also in this case, the coercivity is perpendicular to $H_{c\perp}$ above $H_{c\parallel}$ value for parallel magnetization, indicating the presence of crystallites with large transverse anisotropy lined along the NW. FeNi alloys are of high-permeability, but in nanoscale anisotropy systems may also be due to the form of crystallites. Large transverse anisotropy with an anisotropy field of up to 2.5 kOe was found in FeNi-NW [26]. Data for other diameters are given in Table 3.

As expected, the increase in diameter leads to a decrease in coercivity and residual magnetization for both directions of the magnetic field.

NW made of FeCo alloy. For a single composition NW ($Fe_{0.3}Co_{0.7}$), a study was conducted on the magnetic properties dependence on the diameter. The obtained dependencies (hysteresis loops) for NW samples with diameters of 30, 65 and 100 nm are given in Fig. 5.

It can be seen that for the studied NW there is a significant increase in coercive force with a decrease in the diameter of NW. The maximum value of H_c was obtained for 30 nm diameter samples and was 1300 Oe. FeCo-NW with a crystalline FCC or BCC structure have a small crystalline anisotropy, but may still exhibit a fairly high coercive force because of the anisotropy of the form [27]. In order to achieve high efficiency it is necessary to implement the conditions of single domain state formation, which is possible only at small values of diameter. This explains the maximum values of H_c for the smallest diameter of 30 nm. As the diameter increases, the residual magnetization value decreases at magnetization in the field parallel to the NW length. This may be due to a misalignment of the light magnetization axis with the preferred growth direction, resulting in the reorientation of the magnetocrystalline anisotropy axis away from the NW axis.

Note that the same trend was observed in iron-nickel NW [19]. However, in these cases, there is a different orientation: for FeNi-NW, the H_c values were larger for a field applied perpendicular to the NW axis. By contrast, FeCo-NW H_c was the maximum when the field was applied along the NW. (For example, in sample $Fe_{0.3}Co_{0.7}$ with a diameter of 30 nm H_c it is almost twice as large when the field is applied along the NW axis. At that, the residual magnetization is almost equal to the saturation magnetization). This difference may be due to the different properties of the two materials, as the iron-cobalt sample generally has a higher saturation magnetization than the permalloy sample, resulting in a more pronounced form anisotropy contribution to the overall anisotropy at a reduced diameter.

The study of the dependence of the magnetic properties of FeCo on the composition was continued in [16]. A concentration dependency of H_c was obtained. The second maximum of H_c was confirmed at a Co concentration of about 90%. The latter distinguishes fundamentally the concentration dependence of H_c for NW from the same dependence for bulk material. It can be assumed that the emergence of a second maximum in the NW may be due to the formation of a solid solution based on cobalt.

NW made of FeCo alloy. The main purpose of this step was to obtain a NW with a high value of H_c: it is known that the addition of small amounts of non-magnetic material is used in bulk alloys to increase this parameter. For masses of NW with a diameter of 100 nm and a length of 6 μm the dependence of magnetic properties on the copper content has been studied. Hysteresis loops were measured

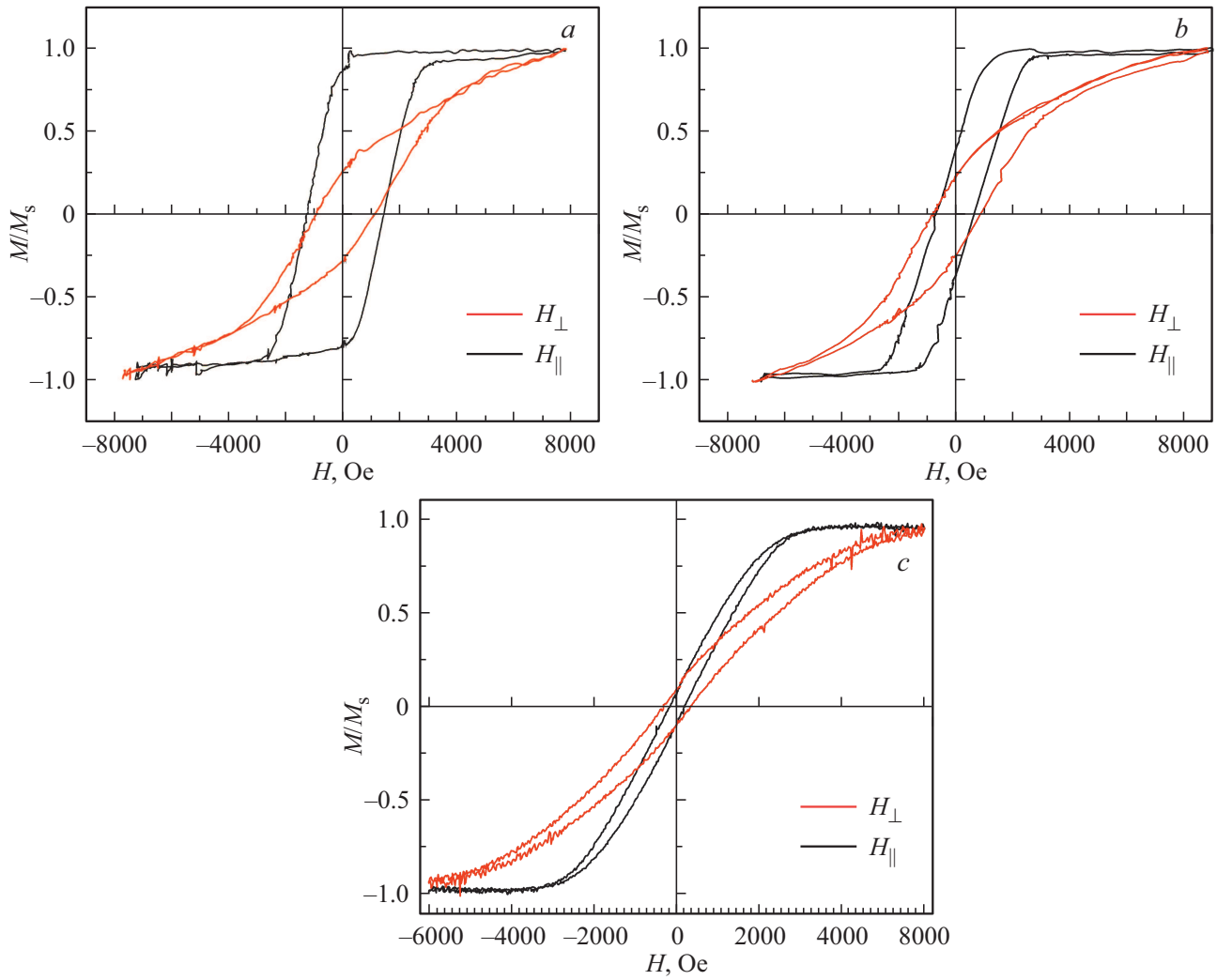

Figure 5. Magnetometer of FeCo alloy NW arrays: hysteresis loop for NW samples with diameter *a* — 30, *b* — 65 and *c* — 100 nm. For each diameter there are graphs for two orientations: in-plane (red curve), out-of-plane (black curve).

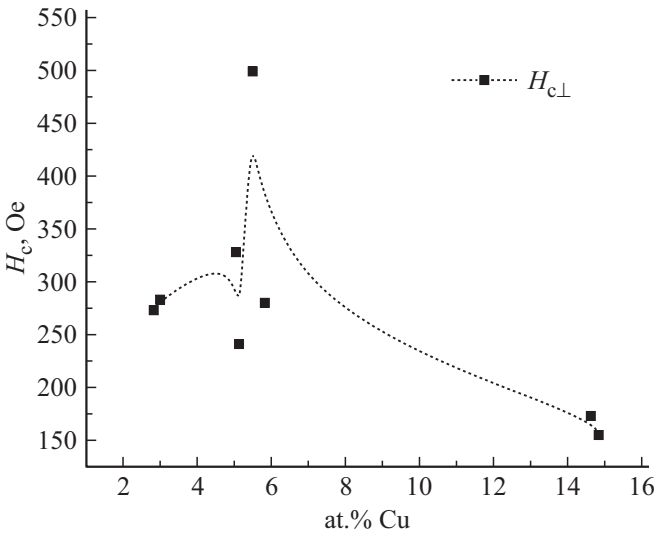

Figure 6. Dependence ofH_c in FeCoCu NW on copper content; measurement in the in-plane geometry.

and the values of H_c were calculated. These dependencies are shown in Fig. 6.

Graphs show a maximum of H_c at a copper content of 5−6%. It is assumed that this is due to the fact that copper under the electrodeposition conditions used forms a separate phase (as confirmed by the preliminary results of X-ray crystallography analysis). This fine-grained phase is an obstacle to domain wall movement, resulting in an increase of H_c.

4. Conclusion

The electrodeposition of NW from double alloys and triple alloys, conducted in a potentiostatic mode, shows a similar nature of dependence of current on time. In all cases, there is an anomalous iron deposition effect. In the case of a triple alloy, the presence of copper changes the ratio of iron to cobalt. Copper deposition is much faster than the deposition of magnetic metals,

resulting in an elevated copper content in the NW. Studies of magnetic properties have shown that H_c in FeNi-NW increases significantly as their diameter decreases. The FeCo-NW also shows a similar relationship: CS increases significantly with a decrease in diameter (up to 1200 Oe with a diameter of 30 nm). When the metal concentration in FeCo-NW changed, two maximums were identified: at equiatomic composition and at cobalt content about 90%, which is a fundamental difference from bulk material. For a triple alloy NW (FeCoCu) it is shown that H_c increases significantly with a copper content of 5−6%. The latter may be due to the formation of a separate fine-crystalline copper phase, the emergence of which is confirmed by preliminary structural data. The results show that there are additional possibilities for producing both soft-magnetic and hard-magnetic materials by regulating the composition and geometry of NW made of alloys.

Acknowledgments

The authors thank prof. P.Yu. Apel (Dubna) for providing track membranes of various types and master's student of MISIS S.A. Lukkareva for assistance in conducting magnetic measurements.

Funding

The work was carried out within the framework of the State Assignment „Crystallography and Photonics“ of RAS and NITU MISIS. The equipment of the IFM RAS Central Research Center was used.

Conflict of interest

The authors declare that they have no conflict of interest.

References

[1] T. Hasegawa, S. Kanatani, M. Kazaana, K. Takahashi, K. Kumagai. Sci. Rep. **7**, *1*, 13215 (2017).
[2] J. Cui, M. Kramer, L. Zhou, F. Liu, A. Gabay, G. Had, B. Bal, D. Sell. Acta Mater. **158**, 118 (2018).
[3] W. Fang, I. Panagiotopoulos, F. Ott, F. Boué, K. Ait-Atmane, J.-Y. Piquemal, G. Viau, F. Dalmas. J. Nanopart. Res. **16**, *2*, 2265 (2014).
[4] K. Gandha, K. Elkins, N. Poudyal, X. Liu, J.P. Liu. Sci. Rep. **4**, 5345 (2014).
[5] Y. Rheem, B.Y. Yoo, B.K. Koo, W.P. Beyermann, N.V. Myung. J. Phys. D **40**, *23*, 7267 (2007).
[6] F.E. Atalay, H. Kaya, S. Atalay, S.J. Tari. Alloys. Compd. **469**, *1−2*, 458 (2009).
[7] S. Dubois, J. Colin, J. Duvail, L. Piraux. Phys. Rev. B **61**, *21*, 14315 (2000).
[8] G. Kartopu, O. Yalçın, K.-L. Choy, R. Topkaya, S. Kazan, B. Aktaş. J. Appl. Phys. **109**, *3*, 033909 (2011).
[9] J. Alonso, H. Khurshid, V. Sankar, Z. Nemati, M.H. Phan, E. Garayo, J.A. Garcia, H. Srikanth. J. Appl. Phys. **117**, *17*, 17D113 (2015).
[10] L. Elbaile, R.D. Crespo, V. Vega, J.A. Garcıa. J. Nanomater. **13**, 198453 (2012).
[11] D.C. Leitao, C.T. Sousa, J. Ventura, J.S. Amaral, F. Carpinteiro, K.R. Pirota, M. Vazquez, J.B. Sousa, J.P. Araujo. J. Non-Crystal. Solids **354**, *47−51*, 5241 (2008).
[12] M. Almasi Kashi, A. Ramazani, S. Doudafkan, A.S. Esmaeily. Appl. Phys. A **102**, *3*, 761 (2011).
[13] K.V. Frolov, D.L. Zagorsky, I.S. Lyubutin, M.A. Chuev, I.V. Perunov, S.A. Bedin, A.A. Lomov, V.V. Artemov, S.N. Sulyanov. Pis'ma v ZhETF **105**, *5*, 297 (2017) (in Russian).
[14] D.L. Zagorsky, K.V. Frolov, S.A. Bedin, I.V. Perunov, M.A. Chuev, A.A. Lomov, I.M. Doludenko. FTT **60**, *11*, 2075 (2018) (in Russian).
[15] K.V. Frolov, M.A. Chuev, I.S. Lyubutin, D.L. Zagorskii, S.A. Bedin, I.V. Perunov, A.A. Lomov, V.V. Artemov, D.N. Khmelenin, S.N. Sulyanova, I.M. Doludenko. J. Magn. Magn. Mater. **489**, 165415 (2019).
[16] I.M. Doludenko, D.L. Zagorsky, K.V. Frolov, I.V. Perunov, M.A. Chuev, V.M. Kanevsky, H.C. Yerokhina, S.A. Bedin. FTT **62**, *9*, 1474 (2020) (in Russian).
[17] D.L. Zagorsky, I.M. Doludenko, V.M. Kanevsky, A.R. Gilimyanova, V.P. Menushenkov, E.S. Savchenko. Izv. RAN. Ser. fiz. **85**, *8*, 1090 (2021) (in Russian).
[18] I.M. Doludenko, D.L. Zagorsky, A.E. Muslimov, L.V. Panina, D.V. Panov, D.R. Khayretdinova, S.A. Lukkareva. Poverkhnost'. Rentgenovskie, sinkhrotronnye i neitronnye issledovaniya, *4*, 58 (2022) (in Russian).
[19] L.V. Panina, S.A. Evstigneeva, P.D. Melnikova, D.R. Khairetdinova, S.A. Lukkareva, A.R. Gilimyanova. Phys. Status Solidi A **219**, *3*, 2100538 (2022).
[20] N. Ahmad, M.Z. Shafiq, S. Khan, W.H. Shah, I. Murtaza, A. Majid, K. Javed. J. Superconductivity. Nov. Magn. **33**, *5*, 1495 (2020).
[21] C. Bran, Yu.P. Ivanov, J. Garcıa, R.P. del Real, V.M. Prida, O. Chubykalo-Fesenko, M. Vazquez. J. Appl. Phys. **114**, *4*, 043908 (2013).
[22] A. Núñez, L. Pérez, M. Abuín, J.P. Araujo, M.P. Proenca. J. Phys. D **50**, *15*, 155003 (2017).
[23] E. Berganza, C. Bran, M. Jaafar, M. Vázquez, A. Asenjo. Sci. Rep. **6**, *1*, 29702 (2016).
[24] P.W. Egolf, N. Shamsudhin, S. Pane, D. Vuarnoz, J. Pokki, A.-G. Pawlowski, P. Tsague, B. de Marco, W. Bovy, S. Tucev, M.H.D. Ansari, B.J. Nelson. J. Appl. Phys. **120**, *6*, 064304 (2016).
[25] I.M. Doludenko. Perspektivnye materialy *8*, 74 (2021) (in Russian).
[26] A.E. Shumskaya, A.L. Kozlovskiy, M.V. Zdorovets, S.A. Evstigneeva, A.V. Trukhanov, S.V. Trukhanov, D.A. Vinnik, E.Yu. Kaniukov, L.V. Panina. J. Alloys. Compd. **810**, 151874 (2019).
[27] K. Gandha, P. Tsai, G. Chaubey, N. Poudyal, K. Elkins, J. Cui, J.P. Liu. Nanotechnol. **26**, *7*, 075601 (2015).